ISSN 1674-1056
http://cpb.iphy.ac.cn
http://iopscience.iop.org/cpb
中国物理 B
Chinese Physics
中国物理
Chinese Physics B

Fringe visibility and distinguishability in two-path interferometer with an asymmetric beam splitter

Yanjun Liu(刘彦军), Jing Lu(卢竞), Zhihui Peng(彭智慧), Lan Zhou(周兰), Dongning Zheng(郑东宁)

Citation: Chin. Phys. B . 2019, 28(3): 030303. **doi:** 10.1088/1674-1056/28/3/030303
Journal homepage: http://cpb.iphy.ac.cn; http://iopscience.iop.org/cpb

What follows is a list of articles you may be interested in

Phase precision of Mach-Zehnder interferometer in PM2.5 air pollution

Duan Xie(谢端), Haifeng Chen(陈海峰)
Chin. Phys. B . 2018, 27(7): 070304. **doi:** 10.1088/1674-1056/27/7/070304

Mach-Zehnder interferometer with squeezed and EPR entangled optical fields

Xu-Dong Xu(于旭东), Wei Li(李卫), Shi-Yao Zhu(朱诗尧), Jing Zhang(张靖)
Chin. Phys. B . 2016, 25(2): 020304. **doi:** 10.1088/1674-1056/25/2/020304

Wave–particle duality in a Raman atom interferometer

Jia Ai-Ai, Yang Jun, Yan Shu-Hua, Hu Qing-Qing, Luo Yu-Kun, Zhu Shi-Yao
Chin. Phys. B . 2015, 24(8): 080302. **doi:** 10.1088/1674-1056/24/8/080302

Elementary analysis of interferometers for wave–particle duality test and the prospect of going beyond the complementarity principle

Li Zhi-Yuan
Chin. Phys. B . 2014, 23(11): 110309. **doi:** 10.1088/1674-1056/23/11/110309

Fringe visibility and distinguishability in two-path interferometer with an asymmetric beam splitter

Yanjun Liu(刘彦军), Jing Lu(卢竞), Zhihui Peng(彭智慧), Lan Zhou(周兰), Dongning Zheng(郑东宁)
Chin. Phys. B . 2019, 28(3): 030303. **doi:** 10.1088/1674-1056/28/3/030303

Fringe visibility and distinguishability in two-path interferometer with an asymmetric beam splitter*

Yanjun Liu(刘彦军)[1,2], Jing Lu(卢竞)[1,†], Zhihui Peng(彭智慧)[1], Lan Zhou(周兰)[1], and Dongning Zheng(郑东宁)[2,3,4]

[1] *Key Laboratory of Low-Dimensional Quantum Structures and Quantum Control of Ministry of Education, Department of Physics and Synergetic Innovation Center of Quantum Effects and Applications, Hunan Normal University, Changsha* 410081, *China*

[2] *Beijing National Laboratory for Condnesed Matter Physics and Institute of Physics, Beijing* 100190, *China*

[3] *CAS Center for Excellence in Topological Quantum Computation and School of Physical Sciences, University of Chinese Academy of Sciences, Beijing* 100049, *China*

[4] *Songshan Lake Materials Laboratory, Dongguan, Guangdong* 523808, *China*

(Received 24 October 2018; revised manuscript received 20 December 2018; published online 25 February 2019)

We study the fringe visibility and the distinguishability of a general Mach–Zehnder interferometer with an asymmetric beam splitter. Both the fringe visibility V and the distinguishability D are affected by the input state of the particle characterized by the Bloch vector $\boldsymbol{S} = (\boldsymbol{S}_x, \boldsymbol{S}_y, \boldsymbol{S}_z)$ and the second asymmetric beam splitter characterized by the paramter β. For the total system is initially in a pure state, it is found that the fringe visibility reaches the upper bound and the distinguishability reaches the lower bound when $\cos\beta = -S_x$. The fringe visibility obtain the maximum only if $S_x = 0$ and $\beta = \pi/2$ when the input particle is initially in a mixed state. The complementary relationship $V^2 + D^2 \leq 1$ is proved in a general Mach–Zehnder interferometer with an asymmetric beam splitter, and the conditions for the equality are also presented.

Keywords: complementarity, fringe visibility, distinguishability, general Mach–Zehnder interferometer

PACS: 03.67.–a, 03.65.Ta, 07.60.Ly **DOI:** 10.1088/1674-1056/28/3/030303

1. Introduction

A single quantum system has mutually exclusive properties, and these characteristics can be converted to each other depending on the method of observation, which is known as Bohr's complementarity principle.[1,2] The well-known example of the complementarity principle is wave-particle duality. A two-path interferometer, such as Young's double slit or Mach–Zehnder interferometer (MZI), is used to quantify the wave-particle duality. The wave-like property and the particle-like property are shown by the fringe visibility and the which-path information (WPI) of the interferometer, respectively.[3–6] If the path of the particle is known accurately, the fringe visibility will disappear. The more WPI is obtained, the less the fringe visibility is shown. Wootters and Zurek[3] proposed the quantitative formulation of the wave-particle duality in the recoiling-slit gedanken experiment. *A priori* fringe visibility V_0 of the interference pattern and the predictability P_0 were first introduced to quantify the wave-particle duality,[4] which satisfied the complementary relationship $V_0^2 + P_0^2 \leq 1$. The inequality $V^2 + D^2 \leq 1$ is derived by Englert in 1996,[6] where V is the fringe visibility and D is the path distinguishability. The inequality $V^2 + D^2 \leq 1$ is also confirmed experimentally.[7] Since the which-path knowledge can be defined in many ways, the complementarity between the fringe visibility and the which-path knowledge has been studied extensively in theory and experiment.[5–29]

The complementary relationship between the fringe visibility and the distinguishability has been obtained in the standard MZI.[6] Later, the complementary relationship in a general MZI with an asymmetric beam splitter (BS) has also attracted great attention.[7,26,29] The asymmetry of the BS1 is equivalent to changing the initial state of the input particles. Since the complementary relationship is established for all the initial state of the input particles, the asymmetry of the BS1 does not affect the complementary relationship. Reference [26] has proposed that additional *a priori* WPI is introduced when the BS2 is asymmetrical. Unlike the symmetric MZI, the fringe visibility obtained at two output ports are different in the general MZI, and the *a priori* WPI is also different when the particle is detected at one or the other output port in the general MZI. In this paper, we study the fringe visibility and the distinguishability in the general MZI with an asymmetric BS. It is found that the magnitudes of fringe visibility and the distinguishability are affected by the asymmetric BS and the input state of the particle. The conditions of the upper bound of the fringe visibility and the lower bound of the distinguishability are also obtained, respectively.

*Project supported by the National Natural Science Foundation of China (Grant Nos. 11434011, 11575058, and 61833010), the "Science and Technology Innovation Platform and Talent Plan" Excellent Talent Award of Hunan Province, China (Grant No. 2017XK2021), the Science Funds from the Ministry of Science and Technology of China (Grant Nos. 2017YFA0304300 and 2016YFA0300601), and the Strategic Priority Research Program of the Chinese Academy of Sciences (Grant No. XDB28000000).

†Corresponding author. E-mail: lujing@hunnu.edu.cn

© 2019 Chinese Physical Society and IOP Publishing Ltd

The paper is organized as follows. In Section 2, we introduce the general MZI with an asymmetric BS, and study the state evolution of the particle and the the detector in the apparatus. In Section 3, we obtain the upper bound of the fringe visibility, and present the condition of obtaining the upper bound. In Section 4, the lower bound of the distinguishability is found, and the condition for obtaining the lower bound is also proposed. In Section 5, we make our conclusion.

2. The apparatus and the state evolution

A general MZI consists of two BSs and two phase shifters (PSs) as shown in Fig. 1. The incident particles are split into two paths by the symmetrical beam splitter BS1. Orthogonal normalized states $|a\rangle$ and $|b\rangle$ are used to denote two possible paths, which support a two-dimensional H_q. When the particles propagate in these two paths, PS1 and PS2 perform an rotation

$$U_{\rm P}(\phi) = \exp(-{\rm i}\phi\sigma_z), \tag{1}$$

on the path qubit, where pauli matrix $\sigma_z = |b\rangle\langle b| - |a\rangle\langle a|$. Finally, these two paths are recombined by the asymmetric beam splitter BS2. The effect of the BS2 on the particles is denoted by

$$U_{\rm B}(\beta) = \exp\left(-{\rm i}\frac{\beta}{2}\sigma_y\right), \tag{2}$$

which is equivalent to performing a rotation around the y axis by angle β. The BS2 is symmetrical when $\beta = \pi/2$.

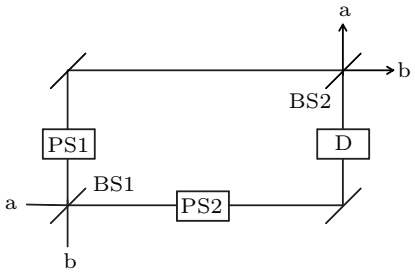


Fig. 1. The schematic sketch of the general Mach–Zehnder interferometer with the second BS asymmetric, and a WPD is placed in path a.

To obtain the WPI, a which-path detector (WPD) is placed on the path a. When a particle is initially in state

$$\rho_{\rm in}^{\rm Q} = \frac{1}{2}(1 + S_x\sigma_x + S_y\sigma_y + S_z\sigma_z), \tag{3}$$

go through the general MZI, the operator $M = |b\rangle\langle b| \otimes I + |a\rangle\langle a| \otimes U$ is performed on the initial state $\rho_{\rm in}^{\rm D}$ of the WPD, where I and U are the identical and unitary operator, respectively. In Eq. (3), the Bloch vector $\boldsymbol{S} = (\boldsymbol{S}_x, \boldsymbol{S}_y, \boldsymbol{S}_z)$. After the particle passes through the general MZI, the state of the particle and the detector becomes

$$\begin{aligned}\rho_{\rm f} &= U_{\rm B}(\beta)MU_{\rm P}(\varphi)U_{\rm B}\left(\frac{\pi}{2}\right)\rho_{\rm in}^{Q}\rho_{\rm in}^{\rm D}U_{\rm B}^{\dagger}\left(\frac{\pi}{2}\right)U_{\rm P}^{\dagger}(\varphi)M^{\dagger}U_{\rm B}^{\dagger}(\beta)\\ &= \frac{1}{4}(1-S_x)(1+\sigma_z\cos\beta+\sigma_x\sin\beta)\otimes\rho_{\rm in}^{\rm D}\\ &\quad -\frac{1}{4}{\rm e}^{-{\rm i}\phi}(S_z-{\rm i}S_y)(\sigma_z\sin\beta-\sigma_x\cos\beta-{\rm i}\sigma_y)\otimes\rho_{\rm in}^{\rm D}U^{\dagger}\\ &\quad -\frac{1}{4}{\rm e}^{{\rm i}\phi}(S_z+{\rm i}S_y)(\sigma_z\sin\beta-\sigma_x\cos\beta+{\rm i}\sigma_y)\otimes U\rho_{\rm in}^{\rm D}\\ &\quad +\frac{1}{4}(1+S_x)(1-\sigma_z\cos\beta-\sigma_x\sin\beta)\otimes U\rho_{\rm in}^{\rm D}U^{\dagger}. \end{aligned}\tag{4}$$

3. Fringe visibility gain via general MZI

The probability that the particle is detected at output port a reads

$$\begin{aligned}p(\phi) &= {\rm tr}_{\rm QD}\left[\frac{1}{2}(1-\sigma_z)\rho_{\rm f}\right]\\ &= \frac{1}{2}(1+S_x\cos\beta)\\ &\quad +\frac{A}{2}\sqrt{\lambda-S_x^2}\sin\beta\cos(\alpha+\gamma+\phi),\end{aligned}\tag{5}$$

where $A = |{\rm tr}_{\rm D}(U\rho_{\rm in}^{\rm D})|$, $S_x^2+S_y^2+S_z^2 = \lambda \le 1$, α and γ are the phases of $S_x + {\rm i}S_y$ and ${\rm tr}_{\rm D}(U\rho_{\rm in}^{\rm D})$, respectively. When $\lambda = 1$, the particle is in a pure state, when $\lambda < 1$, the particle is in a mixed state. The fringe visibility, which characterizes the wave-like property of the particle, is defined via the probability in Eq. (5) as

$$V \equiv \frac{\max{\rm p}(\phi) - \min{\rm p}(\phi)}{\max{\rm p}(\phi) + \min{\rm p}(\phi)} = \frac{A\sin\beta}{1+S_x\cos\beta}\sqrt{\lambda-S_x^2}, \tag{6}$$

where the maximum and the minimum is achieved by adjusting ϕ. We note that the expression of the fringe visibility measured in either output port a or b is different in the general MZI.

Equation (6) shows that the fringe visibility is affected by the initial state of the particle and the BS2. It is found that for a given β, more of the wave's nature appear when the input particle is in a pure state, i.e., $\lambda = 1$. To demonstrate the effect of the initial state of the particle and the BS2 on the fringe visibility, the fringe visibility as a function of the parameter $S_x(\beta)$ for a given $\beta(S_x)$ with $\lambda = 9/25$ or 1 is shown in Fig. 2. In Fig. 2, we have chosen the parameter $A = 1/3$. In Figs. 2(a) (2(c)), we plot the fringe visibility as a function of the parameter S_x for $\lambda = 9/25$ (1) and $\beta = \pi/4$, $\pi/2$, $3\pi/4$ in solid line, dash line, and dotted line. From Figs. 2(a) (2(c)), we can obtain that the fringe visibility first increases and then decreases as S_x increases for a given β. The S_x varies from $-\sqrt{\lambda}$ to $\sqrt{\lambda}$. The value of the fringe visibility is zero when $S_x = \pm\sqrt{\lambda}$, since the particle is determined to propagate only in the path a or the path b, which corresponds to $S_x = \sqrt{\lambda}$ or $-\sqrt{\lambda}$. The position of the peak changes as β changes, and the peak of the fringe visibility appears when $S_x = -\lambda\cos\beta$. For a given β, the change of λ affects the position where the upper bound of the fringe visibility reaches. In Fig. 2(b) (2(d)), we plot the fringe visibility as a function of the parameter β

for $\lambda = 9/25$ (1) and a given S_x. The $S_x = -0.5$, 0, 0.5 are shown by solid line, dash line, and dotted line, respectively. The fringe visibility first increases and then decreases as β increases for a given S_x, as shown in Figs. 2(b) and 2(d). The β varies from 0 to π. The value of the fringe visibility is zero when $\beta = 0$ or π, since the effect of the BS2 for the particle is full transmission or full reflection, which is corresponding to $\beta = 0$ or π. The position of the peak changes as S_x changes, and the peak of the fringe visibility appears when $S_x = -\cos\beta$. Figures 2(b) and 2(d) show that for a given S_x, the change of λ does not affect the position where the upper bound of the fringe visibility reaches. Comparing Figs. 2(a) and 2(c) or Figs. 2(b) and 2(d), we find that when the input particle is initially in a mixed state, the maximum $\sqrt{\lambda}A$ of the fringe visibility is reached only if $S_x = 0$ and $\beta = \pi/2$, i.e., $S_y^2 + S_z^2 = \lambda$ and the BS2 is symmetrical. The maximum A of the fringe visibility is reached when the input particle is initially in a pure state with $S_x = -\cos\beta$. It is also found that the upper bound of the fringe visibility changes as $\beta(S_x)$ changes for a given $S_x(\beta)$ when the input particle is initially in a mixed state, and the upper bound of the fringe visibility does not change as $\beta(S_x)$ changes for a given $S_x(\beta)$ when the input particle is initially in a pure state. To reflect more clearly the conclusions obtained in Fig. 2, we have listed these parameters that make the fringe visibility reach the upper bound in Table 1. Mathematically, by solving the second-order partial derivative of S_x of Eq. (6), it is found that the fringe visibility obtains the upper bound $A\sqrt{\lambda^2 - S_x^2}/\sqrt{\lambda - S_x^2}$ with $S_x = -\lambda\cos\beta$. The fringe visibility reaches the upper bound $A\sqrt{\lambda - S_x^2}/\sqrt{1 - S_x^2}$ with $S_x = -\cos\beta$ by solving the second-order partial derivative of β of Eq. (6). By simple calculations, we can obtain the maximum A of the fringe visibility when the input particle is initially in a pure state with $\cos\beta = -S_x$. It is also found that the fringe visibility obtain the maximum $\sqrt{\lambda}A$ when the input particle is initially in a mixed state, and the maximum is reached only if $S_x = 0$ and $\beta = \pi/2$.

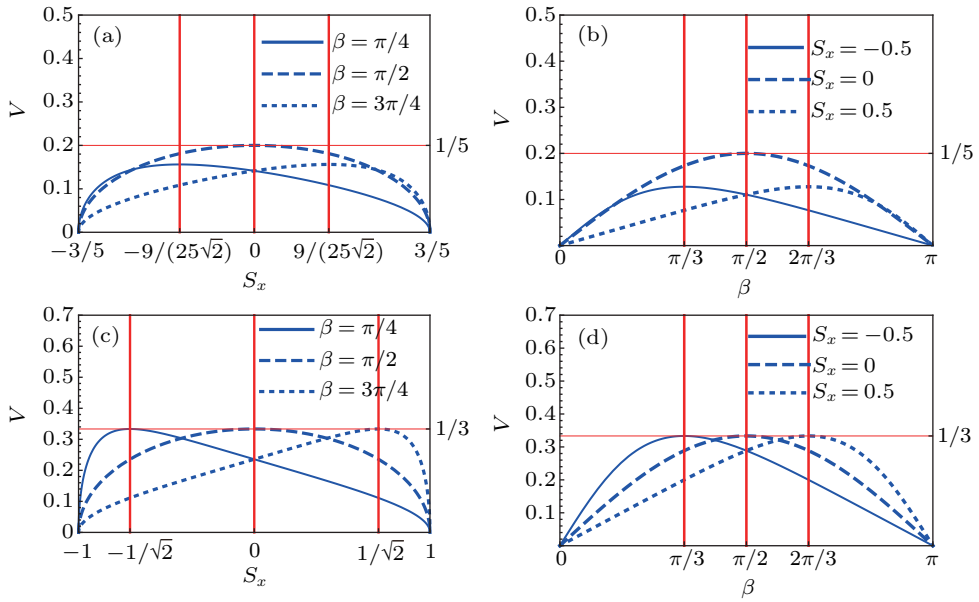


Fig. 2. The fringe visibility as a function of S_x for a given $\beta = \pi/4$ (solid line), $\beta = \pi/2$ (dash line), $\beta = 3\pi/4$ (dotted line) with $\lambda = 9/25$ (a) and $\lambda = 1$ (c). The fringe visibility as a function of β for a given $S_x = -0.5$ (solid line), $S_x = 0$ (dash line), $S_x = 0.5$ (dotted line) with $\lambda = 9/25$ (b) and $\lambda = 1$ (d). Throughout, we have set $A = 1/3$.

Table 1. The maximum of the fringe visibility shown in Fig. 2.

	A	λ	β	S_x	$V_{\max}$
Fig. 2(a)	$\frac{1}{3}$	$\frac{9}{25}$	$\pi/4$	$-9\sqrt{2}/50$	$\sqrt{41}/41$
			$\pi/2$	0	1/5
			$3\pi/4$	$9\sqrt{2}/50$	$\sqrt{41}/41$
Fig. 2(b)	$\frac{1}{3}$		$\pi/3$	$-1/2$	$\sqrt{3}/15$
			$\pi/2$	0	1/5
			$2\pi/3$	1/2	$\sqrt{3}/15$
Fig. 2(c)	$\frac{1}{3}$	1	$\pi/4$	$-\sqrt{2}/2$	$\frac{1}{3}$
			$\pi/2$	0	
			$3\pi/4$	$\sqrt{2}/2$	
Fig. 2(d)	$\frac{1}{3}$		$\pi/3$	$-1/2$	
			$\pi/2$	0	
			$2\pi/3$	1/2	

4. Distinguishability gain via general MZI

To study the particle-like property in the general MZI, the apparatus with four input and output ports has been introduced in Ref. [29]. The state of the WPD was obtained as

$$\rho_{\rm f}^{\rm D} = \omega_{\rm b}\rho_{\rm in}^{\rm D} + \omega_{\rm a}U\rho_{\rm in}^{\rm D}U^{\dagger}, \tag{7}$$

where

$$\omega_{\rm a} = \frac{\cos^2\left(\frac{\beta}{2}\right)(1+S_x)}{1+S_x\cos\beta}, \quad \omega_{\rm b} = \frac{\sin^2\left(\frac{\beta}{2}\right)(1-S_x)}{1+S_x\cos\beta}. \tag{8}$$

We note that the probabilities $\omega_{\rm a}$ and $\omega_{\rm b}$ are only dependent on the parameters S_x and β.

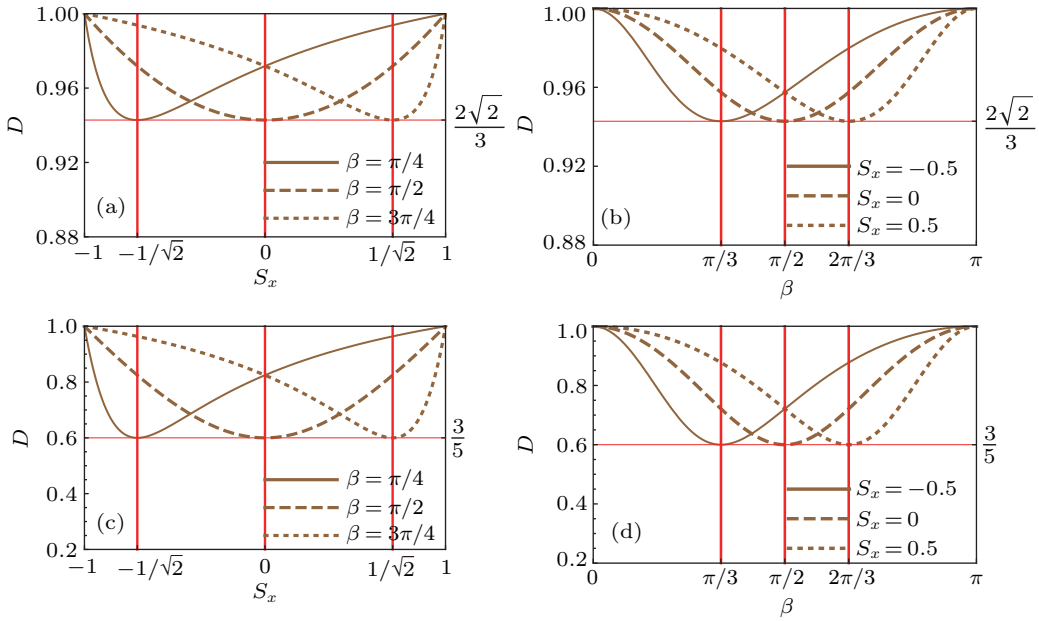


Fig. 3. The distinguishability as a function of S_x for a given $\beta = \pi/4$ (solid line), $\beta = \pi/2$ (dash line), $\beta = 3\pi/4$ (dotted line) with $A = 1/3$ (a) and $A = 4/5$ (c). The distinguishability as a function of β for a given $S_x = -0.5$ (solid line), $S_x = 0$ (dash line), $S_x = 0.5$ (dotted line) with $A = 1/3$ (b) and $A = 4/5$ (d).

The distinguishability, which is used to characterize the particle-like behavior, is introduced by Englert[6]

$$D = \mathrm{Tr_D}\,|\omega_a U \rho_{\mathrm{in}}^{\mathrm{D}} U^{\dagger} - \omega_b \rho_{\mathrm{in}}^{\mathrm{D}}| \leq \sqrt{1 - \frac{\sin^2\beta(1-S_x^2)A^2}{(1+S_x\cos\beta)^2}}. \quad (9)$$

The sign holds in Eq. (9) when the state of the WPD is in a pure state. To obtain the WPI as much as possible, we only study the state of the WPD in a pure state in this section. Here, the magnitude of the distinguishability is determined by the parameters β, S_x, and A. The fringe visibility is determined by all the components of Bloch vector, but only S_x appears in the expression of the distinguishability, indicating that the distinguishability is not dependent on the S_y and S_z . To demonstrate the effect of the initial state of the particle and the BS2 on the distinguishability, the distinguishability as a function of the parameter $S_x(\beta)$ for a given $\beta(S_x)$ with $A = 1/3$ or $4/5$ is shown in Fig. 3. In Fig. 3(a) (3(c)), we plot the distinguishability as a function of the parameter S_x for $A = 1/3$ $(4/5)$ and $\beta = \pi/4, \pi/2, 3\pi/4$ with solid line, dash line, and dotted line. From Figs. 3(a) and 3(c) we can obtain that the distinguishability first decreases and then increases as S_x increases for a given β. The S_x varies from -1 to 1. The value of the distinguishability is 1 when $S_x = \pm 1$, since the particle is determined to propagate only in the path a or the path b, which corresponds to $S_x = 1$ or -1. The position of the valley changes with β, and the valley appears at $S_x = -1/\sqrt{2}$ when $\beta = \pi/4$, $S_x = 0$ when $\beta = \pi/2$, and $S_x = 1/\sqrt{2}$ when $\beta = 3\pi/4$, as shown in Figs. 3(a) and 3(c). Figures 3(a) and 3(c) show that for a given β, the change of A does not affect the position where the lower bound of the distinguishability reaches. In Fig. 3(b) (3(d)), we plot the distinguishability as a function of the parameter β for $A = 1/3$ $(4/5)$ and a given S_x. The $S_x = -0.5$, 0, 0.5 are shown by solid line, dash line, and dotted line, respectively. The distinguishability first decreases and then increases as β increases for a given S_x, as shown in Figs. 3(b) and 3(d). The β varies from 0 to π. The value of the distinguishability is 1 when $\beta = 0$ or π, since the effect of the BS2 for the particle is full transmission or full reflection, which corresponds to $\beta = 0$ or π. The valley appears at $\beta = \pi/3$ when $S_x = -0.5$, $\beta = \pi/2$ when $S_x = 0$, and $\beta = 2\pi/3$ when $S_x = 0.5$, as shown in Figs. 3(b) and 3(d). Figures 3(b) and 3(d) show that for a given S_x, the change of A does not affect the position where the lower bound of the distinguishability reaches. By comparing Figs. 3(a) and 3(c) or Figs. 3(b) and 3(d), we find that the lower bound of the distinguishability is determined by A, and the position of the lower bound is determined by S_x and β. It is also found that the distinguishability obtains the lower bound A when $\cos\beta = -S_x$ (see Fig. 3). To reflect more clearly the conclusions obtained in Fig. 3, we list these parameters that make the distinguishability reach the lower bound in Table 2. Mathematically, we can obtain the minimum $\sqrt{1-A^2}$ of the

Table 2. The minimum of the distinguishability shown in Fig. 3.

	A	β	S_x	$D_{\max}$
Fig. 3(a)	$\frac{1}{3}$	$\pi/4$	$-\sqrt{2}/2$	$2\sqrt{3}/3$
		$\pi/2$	0	
		$3\pi/4$	$\sqrt{2}/2$	
Fig. 3(b)	$\frac{1}{3}$	$\pi/3$	$-1/2$	
		$\pi/2$	0	
		$2\pi/3$	$1/2$	
Fig. 3(c)	$\frac{4}{5}$	$\pi/4$	$-\sqrt{2}/2$	$3/5$
		$\pi/2$	0	
		$3\pi/4$	$\sqrt{2}/2$	
Fig. 3(d)	$\frac{4}{5}$	$\pi/3$	$-1/2$	
		$\pi/2$	0	
		$2\pi/3$	$1/2$	

distinguishability when $\cos\beta = -S_x$ by solving the second-order partial derivative of S_x or β of Eq. (9).

5. Conclusion

We have investigated the effect of the initial state of the particle and the BS2 on both the fringe visibility and the distinguishability. The fringe visibility obtains the upper bound $A = |\mathrm{tr}_{\mathrm{D}}(U\rho_{\mathrm{in}}^{\mathrm{D}})|$ when the total system is initially in a pure state and $\cos\beta = -S_x$, and the maximum A is determined by the initial state of the detector and the unitary operator performed on it. The upper bound of the fringe visibility is related to A, λ, and S_x when the input particle is initially in a mixed state, and the condition for obtaining the upper bound of the fringe visibility for a given β is different from that obtained for a given S_x. The fringe visibility obtains the maximum $\sqrt{\lambda}A$ when the input particle is initially in a mixed state, and the maximum is reached only if $S_x = 0$ and $\beta = \pi/2$. The lower bound $\sqrt{1-A^2}$ of the distinguishability can be achieved when $\cos\beta = -S_x$. We find that the lower bound of the distinguishability is determined by A, and the position of the lower bound are determined by S_x and β. From Eqs. (6) and (9), we obtain the complementary relationship $V^2 + D^2 = 1 - [A^2\sin^2\beta\,(1-\lambda)]/(1+S_x\cos\beta)^2$ when the initially detector is in a pure state and the state of the initially particle is arbitrary. $[A^2\sin^2\beta\,(1-\lambda)]/(1+S_x\cos\beta)^2 = 0$ in the following situations. (i) The effect of the BS2 for the particle is full transmission or full reflection, which is corresponding to $\beta = 0$ or π. (ii) The state of the input particle is in a pure state, which corresponds to $\lambda = 1$. (iii) The states of the detector $|r\rangle$ and $|s\rangle$ are orthogonal state, which corresponds to $A = 0$.

References

[1] Bohr N 1928 *Naturwissenschaften* **16** 245
[2] Bohr N 1928 *Nature* **121** 580
[3] Wootters W K and Zurek W H 1979 *Phys. Rev. D* **19** 473
[4] Greenberger D M and Yasin A 1988 *Phys. Lett. A* **128** 391
[5] Jaeger G, Shimony A and Vaidman L 1995 *Phys. Rev. A* **51** 54
[6] Englert B G 1996 *Phys. Rev. Lett.* **77** 2154
[7] Jacques V, Wu E, Grosshans F, Treussart F, Grangier P, Aspect A and Roch J F 2008 *Phys. Rev. Lett.* **100** 220402
[8] Mandel L 1991 *Opt. Lett.* **16** 1882
[9] Jaeger G, Horne M A and Shimony A 1993 *Phys. Rev. A* **48** 1023
[10] Dürr S, Nonn T and Rempe G 1998 *Phys. Rev. Lett.* **81** 5705
[11] Dörr S 2001 *Phys. Rev. A* **64** 042113
[12] Zawisky M, Baron M and Loidl R 2002 *Phys. Rev. A* **66** 063608
[13] Kaszlikowski D, Kwek L C, Zukowski M and Englert B 2003 *Phys. Rev. Lett.* **91** 037901
[14] Bimonte G and Musto R 2003 *Phys. Rev. A* **67** 066101
[15] Bramon A, Garbarino G and Hiesmayr B C 2004 *Phys. Rev. A* **69** 022112
[16] Peng X H, Zhu X W, Dieter S, Du J F, Liu M L and Gao K L 2005 *Phys. Rev. A* **72** 052109
[17] Jakob M and Bergou J 2007 *Phys. Rev. A* **76** 052107
[18] Ban M J 2008 *Mod. Opt.* **55** 3625
[19] Liu N L, Li L, Yu S X and Chen Z B 2009 *Phys. Rev. A* **79** 052108
[20] Bana M, Shibataa F and Kitajimaa S 2009 *J. Mod. Opt.* **56** 89
[21] Han Y, Wu C W, Wu W, Chen P X and Li C Z 2009 *Chin. Phys. Lett.* **26** 040303
[22] Fonseca-Romero K M, de Oliveira J G G, Peixoto de Faria J G and Nemes M C 2014 *Phys. Rev. A* **90** 062102
[23] Siddiqui M A and Qureshi T 2015 *Prog. Theor. Exp. Phys.* **2015** 083A02
[24] Angelo R M and Ribeiro A D 2015 *Found. Phys.* **45** 1407
[25] Siddiqui M A and Qureshi T 2016 *Quantum Stud.: Math. Found* **3** 115
[26] Li L, Liu N L and Yu S X 2012 *Phys. Rev. A* **85** 054101
[27] Jia A A, Huang J H, Feng W, Zhang T C and Zhu S Y 2014 *Chin. Phys. B* **23** 030307
[28] Jia A A, Yang J, Yan S H, Hu Q Q, Luo Y K and Zhu S Y 2015 *Chin. Phys. B* **24** 080302
[29] Liu Y J, Lu J and Zhou L 2017 *Laser Phys. Lett.* **14** 055204